Highly Stable Anodic Electrochromic Aromatic Polyamides Containing *N*,*N*,*N*′,*N*′-Tetraphenyl-*p*-Phenylenediamine Moieties: Synthesis, Electrochemical, and Electrochromic Properties

Guey-Sheng Liou*,† and Cha-Wen Chang‡

Institute of Polymer Science and Engineering, National Taiwan University, Taipei, 10617, Taiwan, Republic of China, and Department of Applied Chemistry, National Chi Nan University, 1 University Road, Nantou Hsien 54561, Taiwan, Republic of China

Received September 26, 2007; Revised Manuscript Received December 20, 2007

ABSTRACT: A new triphenylamine-containing aromatic diamine, *N*,*N*-bis(4-aminophenyl)-*N*′,*N*′-di(4-methoxylphenyl)-1,4-phenylenediamine (**4**), was successfully synthesized by the cesium fluoride-mediated condensation of 4-amino-4′,4″-dimethoxytriphenylamine with 4-fluoronitrobenzene, followed by palladium-catalyzed hydrazine reduction of the dinitro intermediate. A series of novel polyamides with pendent 4,4′-dimethoxy-substituted triphenylamine (TPA) units having inherent viscosities of 0.28−0.80 dL/g were prepared via the direct phosphorylation polycondensation from the diamine (**4**) and various dicarboxylic acids. All the polymers were amorphous with good solubility in many organic solvents, such as *N*-methyl-2-pyrrolidinone (NMP) and *N*,*N*-dimethylacetamide (DMAc), and could be solution-cast into tough and flexible polymer films. These aromatic polyamides had useful levels of thermal stability associated with their relatively high softening temperature (242−282 °C), 10% weight-loss temperatures in excess of 510 °C, and char yields at 800 °C in nitrogen higher than 63%. The hole-transporting and electrochromic properties are examined by electrochemical and spectroelectrochemical methods. Cyclic voltammograms of the polyamide films cast onto an indium−tin oxide (ITO) coated glass substrate exhibited two reversible oxidation redox couples at 0.47−0.51 and 0.82−0.86 V vs Ag/AgCl in acetonitrile solution. The polyamide films revealed excellent stability of electrochromic characteristics, with a color change from colorless or pale yellowish neutral form to green and blue oxidized form at applied potentials ranging from 0.00 to 0.98 V. These anodically polymeric electrochromic materials not only showed excellent reversible electrochromic stability with good coloration efficiency of green (CE = 285 cm^2/C) and blue (CE = 272 cm^2/C) but also exhibited high contrast of optical transmittance change (ΔT %) up to 60% at 430 nm and 73% at 1035 nm for green, and 86% at 850 nm for blue. After over 1000 cyclic switches, the polymer films still exhibited excellent stability of electrochromic characteristics.

Introduction

Electrochromism involves electroactive materials that present a reversible change in optical properties when the material is electrochemically oxidized or reduced. The electrochromic material exhibit several colors and be termed polyelectrochromic.[1] This interesting property led to the development of many technological applications such as automatic antiglazing mirrors,[2] smart windows,[3] electrochromic displays,[4] and chameleon materials.[5] Triphenylamine- (TPA-) based polymers are not only widely used as the hole−transport layer in electroluminescent devices, but also show interesting electrochromic behavior.[6] Therefore, the intramolecular electron transfer and electronic coupling effects in the oxidized states are important in the design of new TPA-based polymers for electrochromic devices.

Intramolecular electron transfer (ET) processes have been studied extensively in the mixed-valence (MV) systems.[7−9] They usually employed one-dimensional MV compounds contain two or more redox states connected via σ- or π-bridge molecule. The interest in pure organic MV systems is currently increasing,[8,9] especially for the diamine derivatives. For example, Nelsen and co-workers[10] studied a number of *p*-phenylenediamine cation radicals using both the time-dependent theory and spectroscopic measurements. According to Robin and Day,[11] MV systems can be classified into three categories: class I with practically no coupling between the different redox states, class II with moderate electronic coupling, and class III with strong electronic coupling (the electron is delocalized over the two redox centers). Recently, an experimental and theoretical study of the *N*,*N*,*N*′,*N*′-tetraphenyl-*p*-phenylenediamine cation radical has been reported and a symmetrical delocalized class III structure was proposed.[12]

The anodic oxidation pathways of TPA were also well studied.[13] The electrogenerated cation radical of $TPA^{+\bullet}$ is not stable and could dimerize to form tetraphenylbenzidine by tail to tail coupling with loss of two protons per dimer. When the phenyl groups were incorporated by electron-donating substituents at the para-position of TPA, the coupling reactions were greatly prevented by affording stable cationic radicals and lowering the oxidation potenials.[14−17] The redox properties, ion-transfer process, electrochromism, and photoelectrochemical behavior of *N*,*N*,*N*′,*N*′-tetrasubstituted-1,4-phenylenediamines are important for technological application.[18−22] A new material with longer life, higher efficiency, and appropriate highest occupied molecular orbital (HOMO) energy level is in increasing demand. Intensive research efforts have been focused on the development of new charge-transport polymers since they promise a number of commercial advantages over low-molecular-weight counterparts.[23−25] One of the perceived advantages is that polymer films can be more easily deposited over a larger area and they are often flexible. Furthermore, prevention of crystallization and phase-separation may improve the device

* Corresponding author. E-mail: gsliou@ntu.edu.tw.
† Institute of Polymer Science and Engineering, National Taiwan University.
‡ Department of Applied Chemistry, National Chi Nan University.

10.1021/ma702146h CCC: $40.75
Published on Web 02/09/2008

performance. Recently, we have initiated a study to obtain TPA-containing anodic electrochromic polymers which exhibited green and blue color in the oxidized state and were transparent in the neutral state.[26−29]

In this article, we therefore synthesized new diamine, *N*,*N*-bis(4-aminophenyl)-*N*′,*N*′-di(4-methoxyphenyl)-1,4-phenylenediamine (**4**), and its derived polyamides containing TPA groups with an electron-rich pendent 4-methoxy phenyl ring which permits tuning the solubility and redox potential of the polymers. The general properties such as solubility and thermal properties are described. The electrochemical and electrochromic properties of these polymers are also described herein and are compared with those of structurally related ones from *N*,*N*-bis(4-aminophenyl)-*N*′,*N*′-diphenyl-1,4-phenylenediamine.[27]

Experimental Section

Materials. *N*,*N*-Bis(4-aminophenyl)-*N*′,*N*′-diphenyl-1,4-phenylenediamine (mp = 245−247 °C) was synthesized by hydrazine Pd/C-catalyzed reduction of *N*,*N*-bis(4-nitrophenyl)-*N*′,*N*′-diphenyl-1,4-phenylenediamine resulting from the condensation of 4-aminotriphenylamine with 4-fluoronitrobezene in the presence of cesium fluoride (CsF) according to a previously reported procedure.[26] 4-iodoanisole (ACROS), 4-nitroaniline (ACROS), potassuim carbonate (ACROS), copper powder (ACROS), 18-crown-6-ether (TCI), *o*-dichloribezene (TEDIA), *N*,*N*-dimethylacetamide (DMAc) (TEDIA), *N*,*N*-dimethylformamide (DMF) (ACROS), dimethyl sulfoxide (DMSO) (TEDIA), *N*-methyl-2-pyrrolidinone (NMP) (TEDIA), pyridine (Py) (TEDIA), and triphenyl phosphite (TPP) (ACROS) were used without further purification. Commercially available dicarboxylic acids such as succinic acid (**5a**) (Acros), trans-1,4-cyclohexanedicarboxylic acid (**5b**), terephthalic acid (**5c**), isophthalic acid (**5d**), 2,6-naphthalenedicarboxylic acid (**5e**), 4,4′-biphenyldicarboxylic acid (**5f**), 4,4′-oxydibenzoic acid (**5g**), 4,4′-sulfonyldibenzoic acid (**5h**), and 2,2-bis(4-carboxyphenyl)hexafluoropropane (**5i**) were purchased from TCI and used as received. Tetrabutylammonium perchlorate (TBAP) (ACROS) were recrystallized twice by ethyl acetate under nitrogen atmosphere and then dried *in vacuo* prior to use. All other reagents were used as received from commercial sources.

Preparation of the Films. A solution of the polymer was made by dissolving about 0.50 g of the polyamide sample in 10 mL of DMAc. The homogeneous solution was poured into a 9 cm glass Petri dish, which was placed in a 90 °C oven for 3 h to remove most of the solvent; then the semidried film was further dried *in vacuo* at 170 °C for 7 h. The obtained films were about 40−60 μm thick and were used for X-ray diffraction measurements, solubility tests, and thermal analyses.

Measurements. Infrared spectra were recorded on a Perkin-Elmer RXI FT-IR spectrometer. Elemental analyses were run in an Elementar Vario EL-III. ^{1}H and ^{13}C NMR spectra were measured on a Bruker AV-300 and 400 FT-NMR system, and referenced to the $CDCl_3$-d_1, DMSO-d_6 signal, and peak multiplicity was reported as follows: s, singlet; d, doublet. The inherent viscosities were determined at 0.5 g/dL concentration using Tamson TV-2000 viscometer at 30 °C. Wide-angle X-ray diffraction (WAXD) measurements were performed at room temperature (ca. 25 °C) on a Shimadzu XRD-7000 X-ray diffractometer (40 kV, 20 mA), using graphite-monochromatized Cu Kα radiation. Ultraviolet−visible (UV−vis) spectra of the polymers were recorded on a Varian Cary 50 Probe spectrometer. Thermogravimetric analysis (TGA) was conducted with a Perkin-Elmer Pyris 1 TGA. Experiments were carried out on approximately 4−6 mg film samples heated in flowing nitrogen or air (flow rate = 30 cm^3/min) at a heating rate of 20 °C/min. Thermomechanical analysis (TMA) was conducted with a Perkin-Elmer TMA 7 instrument. The TMA experiments were conducted from 50 to 350 °C at a scan rate of 10 °C/min with a penetration probe 1.0 mm in diameter under an applied constant load of 50 mN. Softening temperatures (T_s's) were taken as the onset temperatures of probe displacement on the TMA traces. Cyclic voltammetry was performed with a Bioanalytical System model CV-27 potentiostat and a BAS X−Y recorder with ITO (polymer films area about 0.7 cm × 0.7 cm) was used as a working electrode and a platinum wire as an auxiliary electrode at a scan rate of 50 mV/s against a Ag/AgCl reference electrode in a solution of 0.1 M tetrabutylammonium perchlorate (TBAP)/acetonitrile (CH_3CN). Voltammograms are presented with the positive potential pointing to the left and with increasing anodic currents pointing downward. The spectroelectrochemical cell was composed of a 1 cm cuvette, ITO as a working electrode, a platinum wire as an auxiliary electrode, and a Ag/AgCl reference electrode. Absorption spectra in spectroelectrochemical analysis were measured with a HP 8453 UV−visible spectrophotometer. Photoluminescence spectra were measured with a Jasco FP-6300 spectrofluorometer. Fluorescence quantum yields (Φ_F) values of the samples in NMP were measured by using quinine sulfate in 1 N H_2SO_4 as a reference standard (Φ_F = 0.546).[25,30] All corrected fluorescence excitation spectra were found to be equivalent to their respective absorption spectra.

Results and Discussion

Monomer Synthesis. 4-Amino-4′,4′′-dimethoxytriphenylamine (**2**) was prepared by the potassium carbonate-mediated aromatic nucleophilic substitution reaction of 4-nitroaniline with iodoanisole[31] followed by hydrazine Pd/C-catalytic reduction according to the synthetic route outlined in Scheme 1. The new aromatic diamine *N*,*N*-bis(4-aminophenyl)-*N*′,*N*′-di(4-methoxyphenyl)-1,4-phenylenediamine (**4**), having a bulky pendent 4,4′-dimethoxy-substituted triphenylamine (TPA) group, was successfully synthesized by hydrazine Pd/C-catalyzed reduction of the dinitro compound (**3**) resulting from double N-arylation reaction of compound (**2**) with 4-fluoronitrobenzene in the presence of cesium fluoride. Elemental analysis, IR, and ^{1}H and ^{13}C NMR spectroscopic techniques were used to identify structures of the intermediate compounds (**1**, **2**, and **3**) and the target diamine monomer (**4**). Figure S1 illustrates the ^{1}H and ^{13}C NMR spectra of the diamine monomer (**4**). Assignments of each carbon and proton are assisted by the two-dimensional NMR spectra shown in Figure S2 and the spectra agree well with the proposed molecular structure of compound **4**. The ^{1}H NMR spectra confirm that the nitro groups have been completely transformed into amino groups by the high field shift of the aromatic protons and the resonance signals at around 4.9 ppm corresponding to the amino protons.

Polymer Synthesis. According to the phosphorylation technique first described by Yamazaki and co-workers,[32,33] a series of novel polyamides (**6a**−**6i**) with pendent 4,4′-dimethoxy-substituted triphenylamine units were synthesized from the diamine (**4**) and various dicarboxylic acids *via* solution polycondensation using TPP and Py as condensing agents as shown in Scheme 2. All the polymerization proceeded homogeneously throughout the reaction and afforded clear and highly viscous polymer solutions, which precipitated in a tough, fiberlike form when the resulting polymer solutions were slowly poured into stirring methanol. As shown in Table 1, the obtained polyamides had inherent viscosities in the range of 0.28−0.80 dL/g and could be solution-cast into flexible and tough films, indicating the formation of high molecular weight polymers.

The formation of polyamides was also confirmed by IR and NMR spectroscopy. Figure S3 shows a typical IR spectrum for polyamide **6c**. The characteristic IR absorption bands of the amide group were around 3312 (N−H stretching) and 1654 cm^{-1} (amide carbonyl). Figure S4 shows a typical set of ^{1}H and ^{13}C NMR spectra of polyamide **6c** in DMSO-d_6; all the peaks could be readily assigned to the hydrogen and carbon

Scheme 1. Synthesis of Monomers

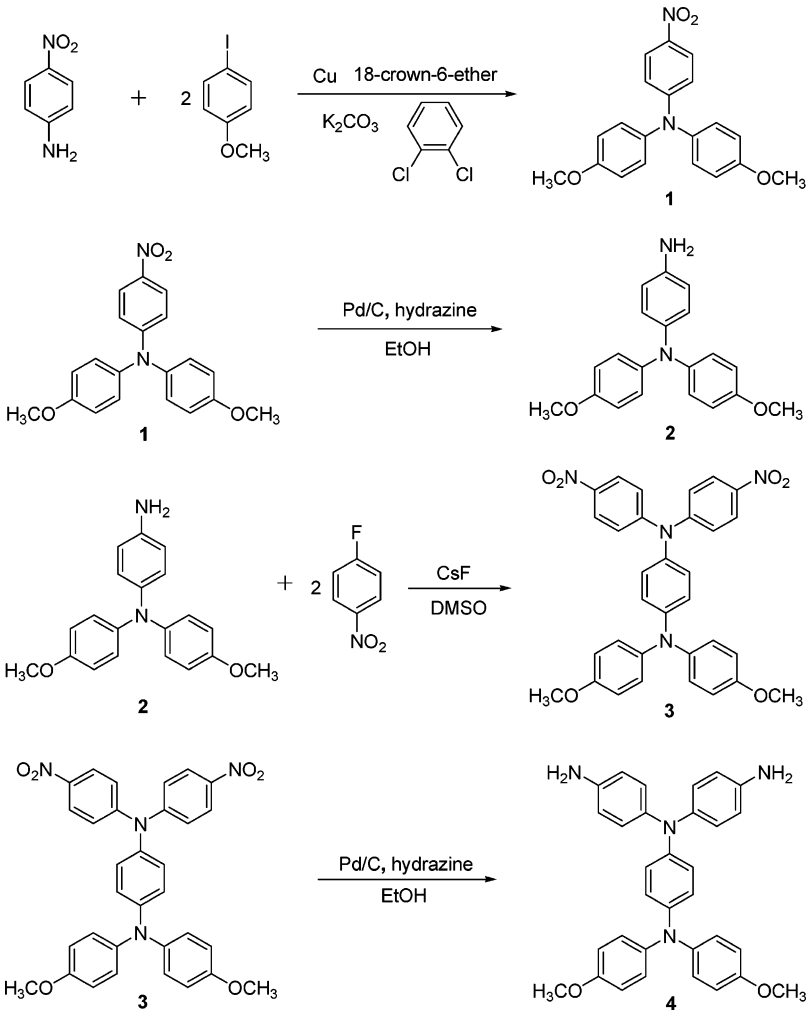

Scheme 2. Synthesis of Polyamides by Direct Polycondesation Reaction

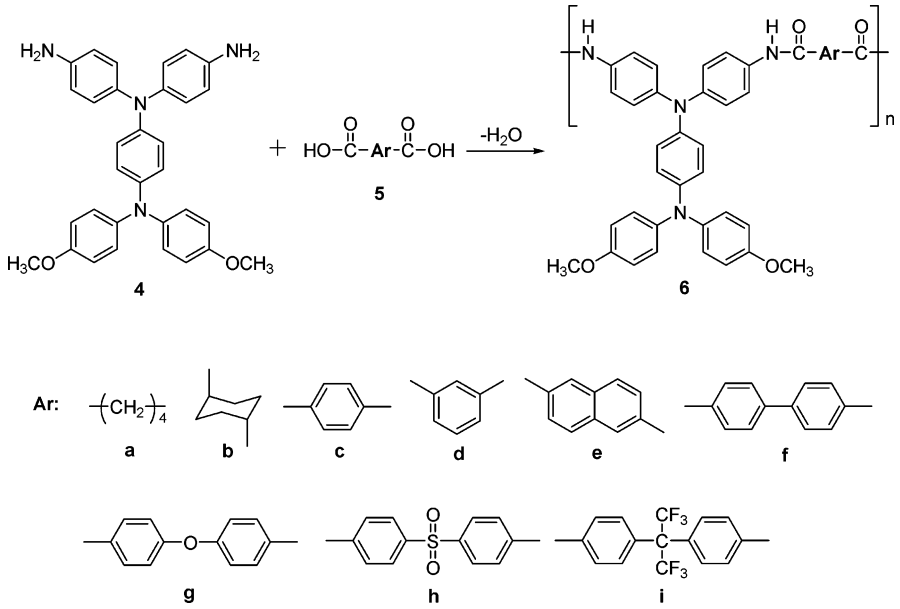

atoms of the recurring unit. Assignments of each carbon and proton are also assisted by the two-dimensional NMR spectra shown in Figure S5 and the spectra agree well with the proposed molecular structure of polyamide **6c**. The resonance peaks appearing at 10.34 ppm in the ^{1}H NMR spectrum and at 164.7 ppm in the ^{13}C NMR spectrum also support the formation of amide linkages.

Basic Characterization. The solubility behavior of polyamides was tested qualitatively, and the results are summarized in Table S1. All the polyamides were highly soluble in polar

Table 1. Inherent Viscosities and Thermal Properties of Polyamides

polymer	η_{inh}[a] (dL/g)	T_g (°C)[b]	T_s (°C)[c]	T_d at 5% weight loss (°C)[d]		T_d at 10% weight loss (°C)[d]		char yield (wt %)[e]
				N_2	air	N_2	air	N_2
6a	0.28	197	190	435	435	455	465	46
6b	0.61	308	299	455	410	480	455	53
6c	0.37	267	274	485	480	520	525	71
6d	0.31	248	242	480	490	510	540	69
6e	0.49	266	255	495	500	530	550	71
6f	0.80	282	282	470	500	520	550	68
6g	0.60	248	233	495	490	530	540	67
6h	0.33	269	259	480	485	510	525	63
6i	0.40	273	263	490	490	525	545	64

[a] Measured at a polymer concentration of 0.5 g/dL in NMP at 30 °C. [b] Midpoint temperature of the baseline shift on the second DSC heating trace (rate = 20 °C/min) of the sample after quenching from 400 to 50 °C (rate = 200 °C/min) in nitrogen. [c] Softening temperature measured by TMA with a constant applied load of 50 mN at a heating rate of 10 °C/min. [d] Decomposition temperature, recorded *via* TGA at a heating rate of 20 °C/min and a gas-flow rate of 30 cm^3/min. [e] Residual weight percentage at 800 °C in nitrogen.

Table 2. Optical and Electrochemical Properties of the Polyamides

	solution λ (nm)[a]			film λ (nm)				oxidation (V) (vs Ag/AgCl in CH_3CN) first		oxidation (V) (vs Ag/AgCl in CH_3CN) second		HOMO[f] (eV)		LUMO[g] (eV)	
polymer	abs max	PL max[b]	$\Phi_{F(\%)}$[c]	λ_0[d]	abs max	abs onset	PL max[b]	$E_{1/2}$	E_{onset}	$E_{1/2}$	E_g[e] (eV)	$E_{1/2}$	E_{onset}	$E_{1/2}$	E_{onset}
6a	314	422	3.75	380	334	388	434	0.51	0.39	0.82	3.20	4.87	4.75	1.67	1.55
6b	312	422	6.07	381	331	390	432	0.48	0.36	0.84	3.18	4.84	4.72	1.66	1.54
6c	311	443	0.17	445	363	484	–	0.49	0.36	0.86	2.56	4.85	4.72	2.29	2.16
6d	351	452	0.15	421	357	453	–	0.50	0.38	0.82	2.74	4.86	4.74	2.12	2.00
6e	313	434	0.10	445	329	488	–	0.49	0.36	0.86	2.54	4.85	4.72	2.31	2.18
6f	308	444	0.08	441	327	473	–	0.48	0.34	0.84	2.62	4.84	4.70	2.22	2.08
6g	351	485	0.16	408	352	420	–	0.48	0.36	0.84	2.95	4.84	4.72	1.89	1.77
6h	333	439	0.16	455	335	506	–	0.47	0.37	0.85	2.45	4.83	4.73	2.38	2.28
6i	354	451	0.16	411	354	463	–	0.50	0.38	0.86	2.68	4.86	4.74	2.18	2.06
6′g	347	461	0.28	406	347	415	–	0.57	0.44	0.95	2.99	4.93	4.80	1.94	1.81

[a] The polymer concentration was 10^{-5} mol/L in NMP. [b] They were excited at the abs_{max} for both the soild and solution states. – :No discernible PL_{max} was observed. [c] The quantum yield in dilute solution was calculated in an integrating sphere with quinine sulfate as the standard ($\Phi_F = 0.546$). [d] The cutoff wavelength from the UV−vis transmission spectra of polymer films. (thickness: 1−3 μm). [e] The data were calculated from polymer film by the equation: gap = $1240/\lambda_{onset}$. [f] The HOMO energy levels were calculated from cyclic voltammetry and were referenced to ferrocene (4.8 eV). [g] LUMO = HOMO − E_g.

solvents such as NMP, DMAc, DMF, and DMSO, and the enhanced solubility could be attributed to the introduction of the bulky pendent 4,4′-dimethoxy-substituted TPA moiety into the repeat unit. Thus, the excellent solubility makes these polymers potential candidates for practical applications by spin- or dip-coating processes.

The wide-angle X-ray diffraction (WAXD) patterns of the polyamides in Figure S6 indicate that the polymers were essentially amorphous, revealing that the 4,4′-dimethoxy-substituted TPA-containing polyamides do not form a well-packed structure. The amorphous nature of these polyamides was reflected not only in their good solubility but also in the UV−vis data of the polymers. The UV−vis absorption peaks of the polymers do not shift from the solutions to the films, implying that there is no significant $\pi-\pi$ interaction aggregation between the polymer chains.

The thermal properties of the polyamides were investigated by TGA and TMA. The results are summarized Table 1. Typical TGA curves of representative polyamide **6i** in both air and nitrogen atmospheres are shown in Figure 1. All the aromatic polyamides exhibited good thermal stability with insignificant weight loss up to 400 °C in nitrogen. Their 10% weight-loss temperatures in nitrogen and air were recorded at 510−530 and 525−550 °C, respectively. The carbonized residue (char yield) of these aromatic polymers was more than 63% at 800 °C in nitrogen atmosphere. The high char yields of these polymers

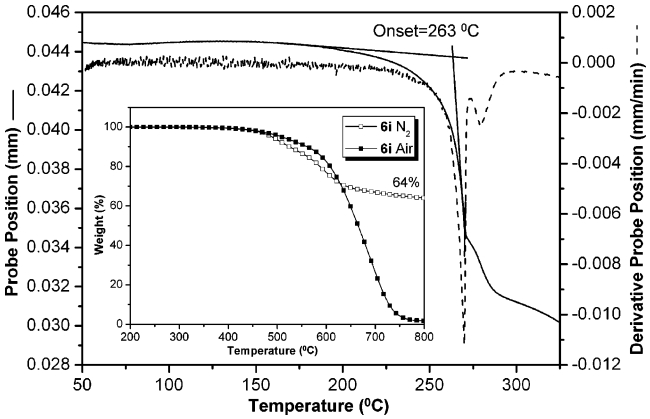

Figure 1. TMA and TGA curve of polyamide **6i** with a heating rate of 10 and 20 °C/min.

could be ascribed to their high aromatic content. The softening temperature (T_s) values of the polymer films were determined from the onset temperature of the probe displacement on the TMA trace. A typical TMA thermogram for polyamide **6i** is illustrated in Figure 1.

Optical and Electrochemical Properties. The optical and electrochemical properties of the polyamides were investigated by UV−vis and photoluminescence spectroscopy, and cyclic voltammetry. The results are summarized in Table 2. The UV−vis absorption of these polymers exhibited strong absorption at

Scheme 3. Simplified Redox Process of Polyamides from Its Neutral State and Radical Cation State to Dication State, Where Coupling Reactions Were Greatly Prevented That Afforded Stable Cationic Radicals

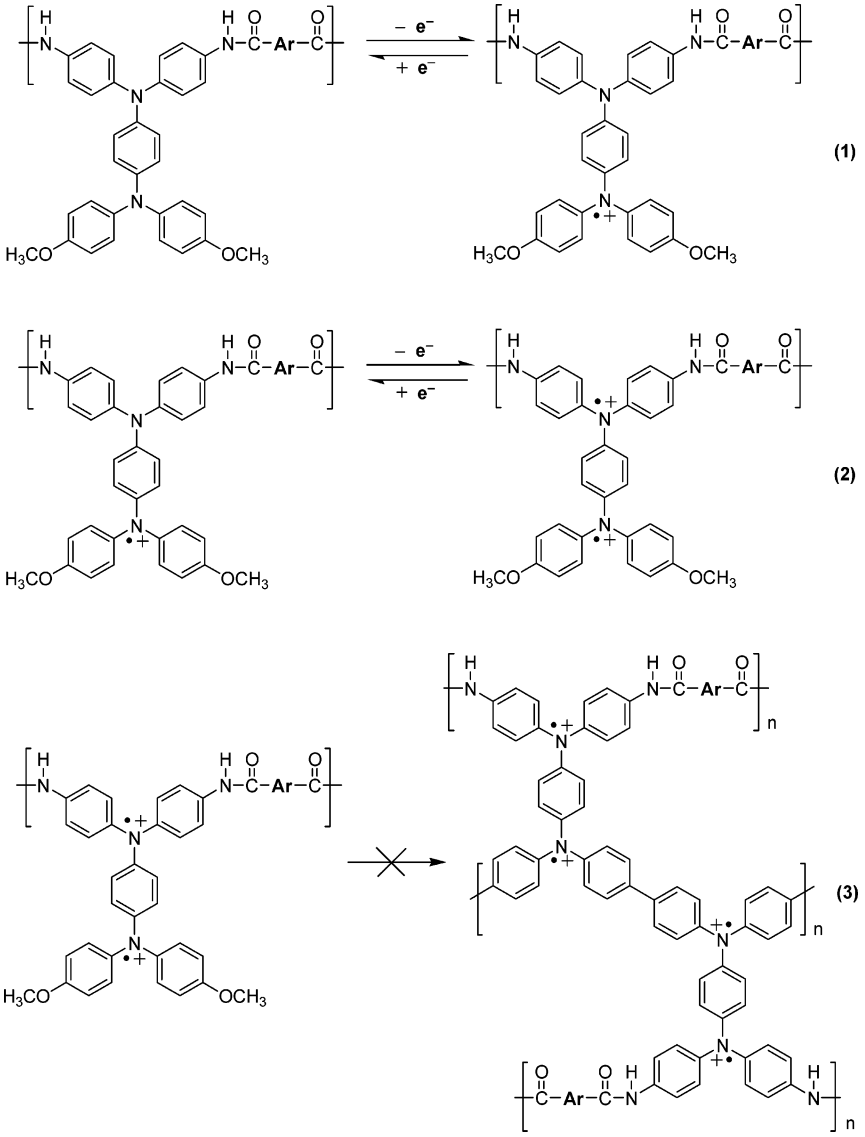

312−354 nm in NMP solutions, which are assignable to a $\pi-\pi^*$ transition resulting from the conjugation between the aromatic rings and nitrogen atoms. The UV−vis absorption of 4,4′-dimethoxy-substituted TPA-based polyamide films **6a**−**6i** also showed similar single absorbance at 331−363 nm. Aromatic−aliphatic polyamides **6a** and **6b** and aromatic polyamides **6c**−**6i** in NMP exhibited fluorescence emission maxima at 422 nm and 434−485 nm with quantum yields ranging from 3.75% for **6a** to 6.07% for **6b**, respectively. The blue shift and higher fluorescence quantum yield of aromatic-aliphatic polyamides **6a** and **6b** compared with aromatic polyamides **6c**−**6i** could be attributed to the effectively reduced conjugation and capability of charge-transfer complex formation by aliphatic diacids with the electron-donating diamine moiety in comparison with that of the stronger electron-accepting aromatic diacids. The cutoff wavelengths (absorption edge) from UV−vis transmittance spectra were in the range of 380−455 nm. Because of the lower capability of charge transfer, polyamides **6a** and **6b** showed a light color and high optical transparency with cutoff wavelengths in the range of 380−381 nm.

The electrochemical behavior of the polyamide **6** series was investigated by cyclic voltammetry conducted by film cast on an ITO-coated glass substrate as the working electrode in dry acetonitrile (CH_3CN) containing 0.1 M of TBAP as an electrolyte under nitrogen atmosphere. The typical cyclic voltammograms for polyamide **6g** (with 4,4′-dimethoxy-substituted) and **6′g** (without 4,4′-dimethoxy-substituted) are shown in Figure 2 for comparison. There are two reversible oxidation redox couples at $E_{1/2}$ values of 0.48 ($E_{onset} = 0.36$) and 0.84 V for polyamide **6g** and 0.57 ($E_{onset} = 0.44$) and 0.95 V for polyamide **6′g** in the oxidative scan. Because of the stability of the films and the good adhesion between the polymer and ITO substrate, polyamide **6g** exhibited excellent reversibility of electrochromic characteristics in 1000 continuous cyclic scans between 0.0 and 0.98 V, changing color from colorless to green and then blue at electrode potentials ranging over 0.48 and 0.84 V. Comparing the electrochemical data, we found that polyamide **6g** was much more easily oxidized than polyamide **6′g** (0.48 vs 0.57 V). The first electron removal for polyamide **6g** was assumed to occur at the N atom on the pendent 4,4′-dimethoxytriphenylamine groups, which was more electron-richer than the N atom on the main chain triphenylamine unit.[27,34] The introduction of electron-donating 4,4′-dimethoxytriphenylamine not only greatly prevent the coupling reaction but also lower the oxidation potentials of the electroactive polyamides **6** as compared with the corresponding polyamides

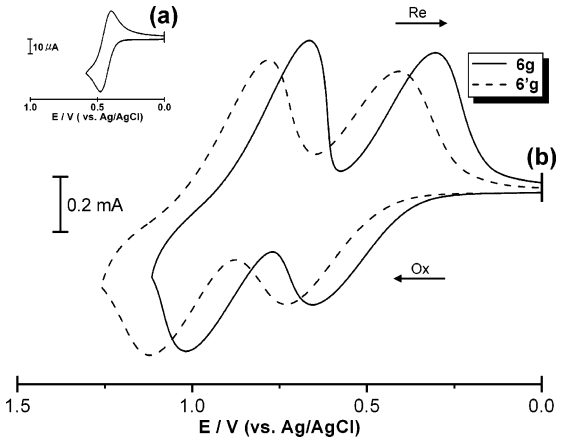

Figure 2. Cyclic voltammograms of polyamides **6g** and **6′g** film onto an indium−tin oxide (ITO)-coated glass substrate in CH_3CN containing 0.1 M TBAP. Scan rate = 0.1 V/s. (a) ferrocene, (b) first and second oxidation redoxs of polyamides **6g** and **6′g.**

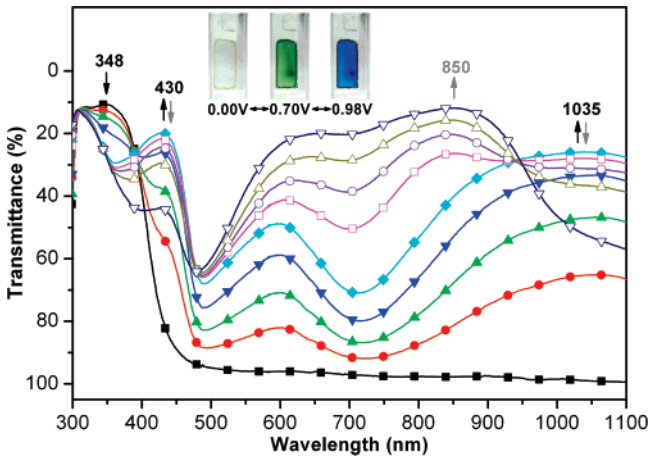

Figure 3. Electorchromic behavior of polyamide **6g** thin film (in CH_3-CN with 0.1 M TBAP As the supporting electrolyte) at 0.00 (■), 0.55 (●), 0.60 (▲), 0.65 (▼), 0.70 (◆),0.80 (□), 0.85 (○), 0.90 (△), and 0.98(▽) (V vs Ag/Ag^+). $\mathbf{6g}^{+\bullet}$: solid symbol with black solid arrow. $\mathbf{6g}^{2+}$: hollow symbol with gray solid arrow.

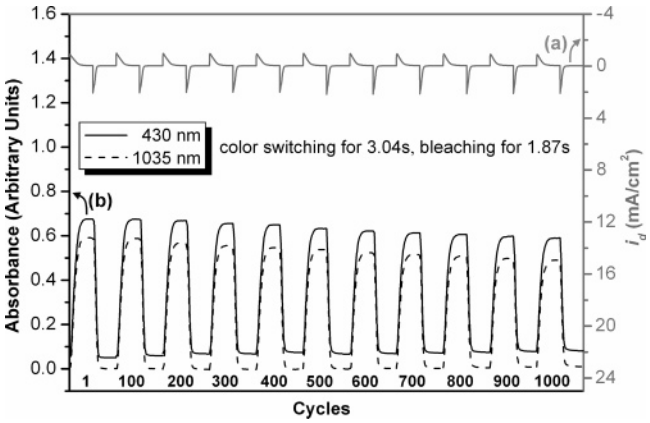

Figure 4. (a) Current consumption and (b) potential step absorptometry of polyamide **6g** (in CH_3CN with 0.1 M TBAP as the supporting electrolyte) by applying a potential step (0.00 V ⇆ 0.70 V), (coated area: 1 cm^2) and cycle time 18s for coloration efficiency from 285 (first cycle) to 269 cm^2/C (1000th cycle).

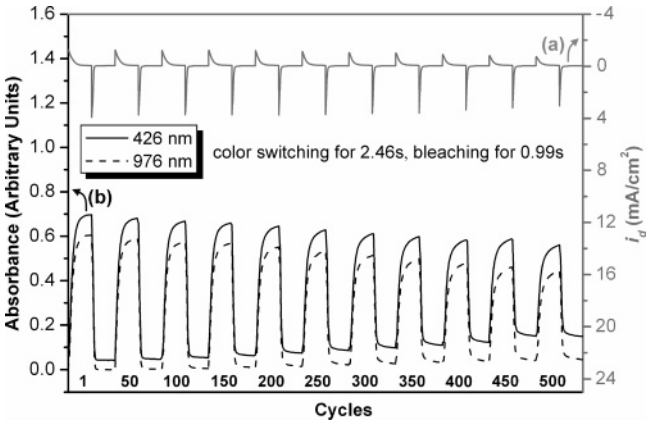

Figure 5. (a) Current consumption and (b) potential step absorptometry of polyamide **6′g** (in CH_3CN with 0.1 M TBAP as the supporting electrolyte) by applying a potential step (0.00 ⇆ 0.75 V), (coated area: 1 cm^2) and cycle time 18 s for coloration efficiency from 271 (first cycle) to 250 cm^2/C (500th cycle).

6′ without methoxyl substituent in Scheme 3. The energy of the highest occupied molecular orbital (HOMO) and lowest unoccupied molecular orbital (LUMO) levels of the investigated polyamides could be determined from the oxidation onset or half-wave potentials and the onset absorption wavelength of polymer films, and the results are listed in Table 2. For example (Figure 2), the oxidation half-wave potential for polyamide **6g** was determined to be 0.48 V (E_{onset} = 0.36 V) vs Ag/AgCl. The external ferrocene/ferrocenium (Fc/Fc^+) redox standard $E_{1/2}$ (Fc/Fc^+) was 0.44 V vs Ag/AgCl in CH_3CN. Under the assumption that the HOMO energy for the ferrocene standard was 4.80 eV with respect to the zero vacuum level, the HOMO energy for polyamide **6g** was evaluated to be 4.84 eV.

Electrochromic Characteristics. Electrochromism of the polyamides thin films was examined by an optically transparent thin-layer electrode (OTTLE) coupled with UV−vis spectroscopy. The electrode preparations and solution conditions were identical to those used in cyclic voltammetry. All these polyamides exhibited similar electrochromic properties, and the typical electrochromic transmittance spectra of polyamide **6g** is shown in Figure 3. When the applied potentials increased positively from 0 to 0.70 V, the peak of transmittance at 348 nm, characteristic for neutral form polyamide **6g** decreased gradually. Two new bands grew up at 430 and 1035 nm due to the first stage oxidation. When the potential was adjusted to a more positive value of 0.98 V, corresponding to the second step oxidation, the peak of characteristic absorbance decreased gradually and one new band grew up at 850 nm. Meanwhile, the film changed from original colorless to green and then to a blue oxidized form. Polymer **6g** exhibited high contrast of optical transmittance change (ΔT %) up to 60% at 430 nm and 73% at 1035 nm for green and 86% at 850 nm for blue (as shown in Figure 3).

The color switching times were estimated by applying a potential step, and the absorbance profiles were followed (Figure 4, S7 for **6g** and Figure 5, S8 for **6′g**). The switching time was defined as the time required for reach 90% of the full change in absorbance after the switching of the potential. Thin film from polyamide **6g** required 3.04 s at 0.70 V for switching absorbance at 430 and 1035 nm and 1.87 s for bleaching. When the potential was set at 0.98 V, thin film **6g** required 4.02 s for coloration at 850 nm and 2.02 s for bleaching. After over 1000 cyclic switches, the films of polyamide **6g** had less ΔOD change than **6′g**. The high electrochromic coloration efficiency of green ($\eta = \Delta OD_{430}/Q$) (285 cm^2/C for 1 cycle to 269 cm^2/C for 1000 cycles) and blue ($\eta = \Delta OD_{850}/Q$) (272 cm^2/C for 1 cycle to 247 cm^2/C for 1000 cycles) of the polyamide **6g** and decay of

Table 3. Optical and Electrochemical Data Collected for Coloration Efficiency Measurements of Polyamides 6g and 6′g

			Q (mC/cm^2)[c]		η (cm^2/C)[d]		decay (%)[e]	
cycles[a]	**6g** ΔOD_{430}[b]	**6′g** ΔOD_{426}[b]	**6g**	**6′g**	**6g**	**6′g**	**6g**	**6′g**
1	0.625 (0.971)[f]	0.655 (0.947)[f]	2.19 (3.57)	2.42 (4.00)	285 (272)	271 (237)	0 (0)	0 (0)
100	0.617 (0.949)	0.614 (0.897)	2.19 (3.51)	2.29 (3.87)	282 (270)	268 (232)	0.1 (0.1)	1.1 (2.1)
200	0.600 (0.933)	0.572 (0.842)	2.17 (3.46)	2.18 (3.73)	276 (270)	262 (226)	3.2 (0.1)	3.3 (4.6)
300	0.588 (0.915)	0.514 (0.765)	2.13 (3.43)	2.01 (3.43)	276 (267)	256 (223)	3.2 (1.8)	5.5 (5.9)
400	0.576 (0.903)	0.461 (0.658)	2.09 (3.42)	1.82 (3.02)	276 (264)	253 (218)	3.2 (2.9)	6.6 (8.0)
500	0.567 (0.889)	0.413 (0.513)	2.06 (3.42)	1.65 (2.42)	275 (260)	250 (212)	3.5 (4.4)	7.7 (10.5)
600	0.554 (0.875)	*g*	2.03 (3.39)		273 (258)		4.2 (5.1)	
700	0.542 (0.861)		1.99 (3.39)		272 (254)		4.6 (6.6)	
800	0.531 (0.846)		1.96 (3.34)		271 (253)		4.9 (7.0)	
900	0.520 (0.828)		1.93 (3.31)		269 (250)		5.6 (8.1)	
1000	0.509 (0.810)		1.89 (3.28)		269 (247)		5.6 (9.2)	

[a] Times of cyclic scan by applying potential steps: 0.00 ↔ 0.70, 0.00 ↔ 0.98 for **6g** and 0.00 ↔ 0.75, 0.00 ↔ 1.08 for **6′g** (V vs Ag/AgCl). [b] Optical density change at 430 nm for **6g** and 426 nm for **6′g.** [c] Ejected charge, determined from the *in situ* experiments. [d] Coloration efficiency is derived from the equation: $\eta = \Delta OD/Q$. [e] Decay of coloration efficiency after cyclic scans. [f] Data in parentheses are optical density change at 850 nm for **6g** and 741 nm for **6′g**. [g] The polyamide **6′g** is not measured after 500 cycles.

the polyamides **6g** and **6′g** were also calculated,[35] and the results are summarized in Table 3.

Conclusions

A series of highly stable anodic green and blue electrochromic polyamides with high contrast of optical transmittance change (ΔT %) up to 60% at 430 nm and 73% at 1035 nm for green and 86% at 850 nm for blue have been readily prepared from the new diamine, *N*,*N*-bis(4-aminophenyl)-*N*′,*N*′-di(4-methoxyphenyl)-1,4-phenylenediamine, and various dicarboxylic acids *via* the direct phosphorylation polycondensation. By incorporating electron-donating methoxy substituents at the para-position of *N*,*N*,*N*′,*N*′-tetraphenyl-1,4-phenylenediamine, not only could the electrochemical oxidative coupling reactions be greatly prevented by affording stable cationic radicals but also the oxidation potentials of the electroactive polyamides were lowered. In addition to enhanced solubility and excellent thin film formability, these anodically polymeric electrochromic materials also showed excellent continuous cyclic stability of electrochromic characteristic with good coloration efficiency of green (285 cm^2/C for 1 cycle to 269 cm^2/C for 1000 cycles) and blue (272 cm^2/C for 1 cycle to 247 cm^2/C for 1000 cycles). The color changes from the colorless or pale yellowish neutral form to the green and blue oxidized forms when scanning potentials positively from 0.00 to 0.98 V. After over 1000 cyclic switches, the polymer films still exhibited excellent reversibility of electrochromic characteristics. Thus, the 4,4′-dimethoxy-substituted TPA-based polyamides could be good candidates as anodic electrochromic materials due to their proper oxidation potentials, excellent electrochemical stability, and thin film formability.

Acknowledgment. The authors are grateful to the National Science Council of the Republic of China for financial support of this work.

Supporting Information Available: Text giving experimental data, including synthesis of the monomers and polymers and diagrams showing their structures, figures showing ^{1}H and ^{13}C NMR spectra, HMQC spectra, IR spectra, WAXD patterns, and current consumption and potential step absorptometry plots and a table giving solubility data. This material is available free of charge via the Internet at http://pubs.acs.org.

References and Notes

(1) Monk, P. M. S.; Mortimer, R. J.; Rosseinsky, D. R. *Electrochromism*: *Fundamentals and Applications*, VCH, Weinheim, Germany, 1995.
(2) Byker, H. J. (Gentex Corp.), U.S. Patent No. 4,902,108.
(3) Mortimer, R. G. *Chem. Soc. Rev.* **1997**, *26*, 147.
(4) (a) Monk, P. M. S. *J. Electroanal. Chem.* **1997**, *432*, 175. (b) Monk, P. M. S. *Handb. Lumin., Disp. Mater., Devices* **2003**, *3*, 261.
(5) (a) Meeker, D. L.; Mudigonda, D. S. K.; Osborn, J. M.; Loveday, D. C.; Ferraris, J. P. *Macromolecules* **1998**, *31*, 2943. (b) Mudigonda, D. S. K.; Meeker, D. L.; Loveday, D. C.; Osborn, J. M.; Ferraris, J. P. *Polymer* **1999**, *40*, 3407. (c) Brotherston, I. D.; Modigonda, D. S. K.; Osborn, J. M.; Belk, J.; Chen, J.; Loveday, D. C.; Boehme, J. L.; Ferraris, J. P.; Meeker, D. L. *Electrochim. Acta* **1999**, *44*, 2993. (d) Beaupré, S.; Dumas, J.; Leclerc, M. *Chem. Mater.* **2006**, *18*, 4011.
(6) (a) Ogino, K.; Kanagae, A.; Yamaguchi, R.; Sato, H.; Kurtaja, J. *Macromol. Rapid Commun.* **1999**, *20*, 103. (b) Yu, W. L.; Pei, J.; Huang, W.; Heeger, A. J. *Chem. Commun.* **2000**, *8*, 681. (c) Chou, M. Y.; Leung, M. K.; Su, Y. O.; Chiang, S. L.; Lin, C. C.; Liu, J. H.; Kuo, C. K.; Mou, C. Y. *Chem. Mater.* **2001**, *16*, 654.
(7) Creutz, C.; Taube, H. *J. Am. Chem. Soc.* **1973**, *95*, 1086.
(8) Lambert, C.; Noll, G. *J. Am. Chem. Soc.* **1999**, *121*, 8434.
(9) Leung, M. K.; Chou, M. Y.; Su, Y. O.; Chiang, C. L.; Chen, H. L.; Yang, C. F.; Yang, C. C.; Lin, C. C.; Chen, H. T. *Org. Lett.* **2003**, *5*, 839.
(10) Bailey, S. E.; Zink, J. I.; Nelsen, S. F. *J. Am. Chem. Soc.* **2003**, *125*, 5939.
(11) Robin, M.; Day, P. *Adv. Inorg. Radiochem.* **1967**, *10*, 247.
(12) Szeghalmi, A. V.; Erdmann, M.; Engel, V.; Schmitt, M.; Amthor, S.; Kriegisch, V.; Noll, G.; Stahl, R.; Lambert, C.; Leusser, D.; Stalke, D.; Zabel, M.; Popp, J. *J. Am. Chem. Soc.* **2004**, *126*, 7834.
(13) Seo, E. T.; Nelson, R. F.; Fritsch, J. M.; Marcoux, L. S.; Leedy, D. W.; Adams, R. N. *J. Am. Chem. Soc.* **1966**, *88*, 3498.
(14) Hagopian, L.; Kohler, G.; Walter, R. I. *J. Phys. Chem.* **1967**, *71*, 2290.
(15) Ito, A.; Ino, H.; Tanaka, K.; Kanemoto, K.; Kato, T. *J. Org. Chem.* **2002**, *67*, 491.
(16) Chiu, K. Y.; Su, T. X.; Li, J. H.; Lin, T. H.; Liou, G. S.; Cheng, S. H. *J. Electroanal. Chem.* **2005**, *575*, 95.
(17) Chang, C. W.; Liou, G. S.; Hsiao, S. H. *J. Mater. Chem.* **2007**, *17*, 1007.
(18) Marken, F.; Hayman, C. M.; Bulman Page, P. C. *Electrochem. Commun.* **2002**, *4*, 462.
(19) Marken, F.; Webster, S. D.; Bull, S. D.; Davies, S. G. *J. Electroanal. Chem.* **1997**, *437*, 209.
(20) Wadhawan, J. D.; Evans, R. G.; Banks, C. E.; Wilkins, S. J.; France, R. R.; Oldham, N. J.; Fairbanks, A. J.; Wood, B.; Walton, D. J.; Schroder, U.; Compton, R. G. *J. Phys. Chem. B* **2002**, *106*, 9619.
(21) Davies, W. B.; Svec, W. A.; Ratner, M. A.; Wasielewski, M. R. *Nature* **1998**, *396*, 60.
(22) Chiu, K. Y.; Su, T. H.; Huang, C. W.; Liou, G. S.; Cheng, S. H. *J. Electroanal. Chem.* **2005**, *578*, 283.
(23) Akcelrud, L. *Prog. Polym. Sci.* **2003**, *28*, 875.
(24) (a) Chen, S. H.; Chen, Y. *J. Polym. Sci. Part A: Polym Chem* **2004**, *42*, 5900. (b) Yang, N. C.; Lee, S. M.; Yoo, Y. M.; Kim, J. K.; Suh, D. H. *J. Polym. Sci. Part A: Polym Chem* **2004**, *42*, 1058.
(25) (a) Pyo, S. M.; Kim, S. I.; Shin, T. J.; Ree, M.; Park, K. H.; Kang, J. S. *Macromolecules* **1998**, *31*, 4777. (b) Kim, J.-S.; Ahn, H. K.; Ree, M. *Tetrahedron Lett.* **2005**, *46*, 277. (c) Pyo, S. M.; Kim, S. I.; Shin, T. J.; Ree, M.; Park, K. H.; Kang, J. S. *Polymer* **1998**, *40*, 125. (d) Shin, T. J.; Park, H. K.; Lee, S. W.; Lee, B.; Oh, W.; Kim, J.-S.; Baek, S.; Hwang, Y.-T.; Kim, H.-C.; Ree, M. *Polym. Eng. Sci.* **2003**, *46*, 1232. (e) Pyo, S. M.; Shin, T. J.; Kim, S. I.; Ree, M. *Mol. Cryst. Liq. Cryst.* **1998**, *316*, 353.

(26) Cheng, S. H.; Hsiao, S. H.; Su, T. H.; Liou, G. S. *Macromolecules* **2005**, *38*, 307.
(27) Su, T. H.; Hsiao, S. H.; Liou, G. S. *J. Polym. Sci., Part A: Polym. Chem.* **2005**, *43*, 2085.
(28) Liou, G. S.; Hsiao, S. H.; Su, T. H. *J. Mater. Chem.* **2005**, *15*, 1812.
(29) Liou, G. S.; Hsiao, S. H.; Su, T. H. *J. Polym. Sci., Part A: Polym. Chem.* **2005**, *43*, 3245.
(30) Demas, J. N.; Crosby, G. A. *J. Phys. Chem.* **1971**, *75*, 991.
(31) Yano, M.; Ishida, Y.; Aoyama, K.; Tatsumi, M.; Sato, K.; Shiomi, D.; Ichimura, A.; Takui, T. *Synth. Met.* **2003**, *137*, 1275.
(32) Yamazaki, N.; Higashi, F.; Kawabata, J. *J. Polym. Sci., Polym. Chem. Ed.* **1974**, *12*, 2149.
(33) Yamazaki, N.; Matsumoto, M.; Higashi, F. *J. Polym. Sci., Polym. Chem. Ed.* **1975**, *13*, 1375.
(34) Nelson, R. F.; Adams, R. N. *J. Am. Chem. Soc.* **1968**, *90*, 3925.
(35) Mortimer, R. J.; Reynolds, J. R. *J. Mater. Chem.* **2005**, *15*, 2226.

MA702146H